AJNR

# Primary Cerebral Lymphoma and Glioblastoma Multiforme: Differences in Diffusion Characteristics Evaluated with Diffusion Tensor Imaging

C.-H. Toh, M. Castillo, A.M.-C. Wong, K.-C. Wei, H.-F. Wong, S.-H. Ng and Y.-L. Wan

This information is current as of September 2, 2025.

*AJNR Am J Neuroradiol* 2008, 29 (3) 471-475
doi: https://doi.org/10.3174/ajnr.A0872
http://www.ajnr.org/content/29/3/471

ORIGINAL RESEARCH

# Primary Cerebral Lymphoma and Glioblastoma Multiforme: Differences in Diffusion Characteristics Evaluated with Diffusion Tensor Imaging

C.-H. Toh
M. Castillo
A.M.-C. Wong
K.-C. Wei
H.-F. Wong
S.-H. Ng
Y.-L. Wan

**BACKGROUND AND PURPOSE:** Differentiating between primary cerebral lymphoma and glioblastoma multiforme (GBM) based on conventional MR imaging sequences may be impossible. Our hypothesis was that there are significant differences in fractional anisotropy (FA) and apparent diffusion coefficient (ADC) between lymphoma and GBM, which will allow for differentiation between them.

**MATERIALS AND METHODS:** Preoperative diffusion tensor imaging (DTI) was performed in 10 patients with lymphoma and 10 patients with GBM. Regions of interest were placed in only solid-enhancing tumor areas and the contralateral normal-appearing white matter (NAWM) to measure the FA and ADC values. The differences in FA and ADC between lymphoma and GBM, as well as between solid-enhancing areas of each tumor type and contralateral NAWM, were analyzed statistically. Cutoff values of FA, FA ratio, ADC, and ADC ratio for distinguishing lymphomas from GBMs were determined by receiver operating characteristic curve analysis.

**RESULTS:** FA and ADC values of lymphoma were significantly decreased compared with NAWM. Mean FA, FA ratio, ADC ($\times 10^{-3}$ mm$^2$/s), and ADC ratios were 0.140 ± 0.024, 0.25 ± 0.04, 0.630 ± 0.155, and 0.83 ± 0.14 for lymphoma, respectively, and 0.229 ± 0.069, 0.40 ± 0.12, 0.963 ± 0.119, and 1.26 ± 0.13 for GBM, respectively. All of the values were significantly different between lymphomas and GBM. Cutoff values to differentiate lymphomas from GBM were 0.192 for FA, 0.33 for FA ratio, 0.818 for ADC, and 1.06 for ADC ratio.

**CONCLUSIONS:** The FA and ADC of primary cerebral lymphoma were significantly lower than those of GBM. DTI is able to differentiate lymphomas from GBM.

Primary cerebral lymphoma represents 4%–7% of primary brain tumors, and its incidence has increased in the last 3 decades.[1] Despite some characteristic conventional MR imaging findings, it may be difficult or even impossible to distinguish cerebral lymphomas from glioblastoma multiforme (GBM).[2] Accurate preoperative differentiation between these 2 tumors is important for the determination of appropriate treatment strategies.

Lymphomas are relatively hyperintense to gray matter on trace diffusion-weighted images (DWIs) and isointense to hypointense on apparent diffusion coefficient (ADC) maps, findings consistent with restricted water diffusion.[3-5] In contrast, high-grade gliomas are relatively hyperintense to gray matter on both trace DWIs and ADC maps, findings consistent with elevated diffusivity.[3,6,7] Prior studies have shown statistically significant differences in ADC between the cerebral lymphoma and GBM.[4,5] However, the GBM with restricted water diffusion, that is, hyperintense on trace images and hypointense on ADC maps, has also been reported.[8-12] Therefore, discrimination of lymphoma from some GBMs may be difficult.

Received June 20, 2007; accepted after revision September 26.

From the Departments of Medical Imaging and Intervention (C.-H.T., A.M.-C.W., H.-F.W., S.-H.N., Y.-L.W.) and Neurosurgery (K.-C.W.), Chang Gung Memorial Hospital and Chang Gung University College of Medicine, Tao-Yuan, Taiwan; Department of Radiology (M.C.), University of North Carolina School of Medicine, Chapel Hill, NC.

Please address correspondence to Cheng-Hong Toh, Department of Medical Imaging and Intervention, Chang Gung Memorial Hospital, and Chang Gung University College of Medicine, 5 Fu Hsing St, Kwei Shan Hsiang, Tao-Yuan 333, Taiwan; e-mail: eldomtoh@hotmail.com

DOI 10.3174/ajnr.A0872

Diffusion tensor imaging (DTI) provides a sensitive means to detect alterations in the integrity of white matter structures.[13,14] Fractional anisotropy (FA) is a quantitative index for diffusion anisotropy that correlates with microstructural integrity of myelinated fiber tracts.[15,16] FA decreases in a wide variety of intracranial pathologies including brain tumors.[17-20] Previous studies found significant FA differences in tumors with different histologic grades or cellularity.[20-23] FA was also reported to have a strong correlation with cellularity.[20] Because the cellularity of lymphoma is higher than that of GBM, we hypothesized that the diffusion characteristics of lymphoma and GBM are different on DTI and will allow us to differentiate between the two.

## Materials and Methods

### *Patients*

Approval for this study was obtained from the institutional board of research associates. Signed informed consent was obtained from all of the patients. Patient identifiers were removed from image data before analysis. MR examinations were performed in 10 patients (4 men and 6 women; mean age, 53.3 years; age range, 22–75 years) with biopsy-proven primary cerebral lymphomas and 10 patients (5 men and 5 women; mean age, 51.9 years; age range, 23–80 years) with biopsy-proven GBMs (WHO grade IV). None of the patients had begun corticosteroid treatment, radiation therapy, or chemotherapy or had had a previous brain biopsy at the time of MR imaging.

### *MR Imaging*

All of the patients underwent MR imaging, including axial T2-weighted (turbo spin-echo), DWI, DTI, and axial spin-echo T1-

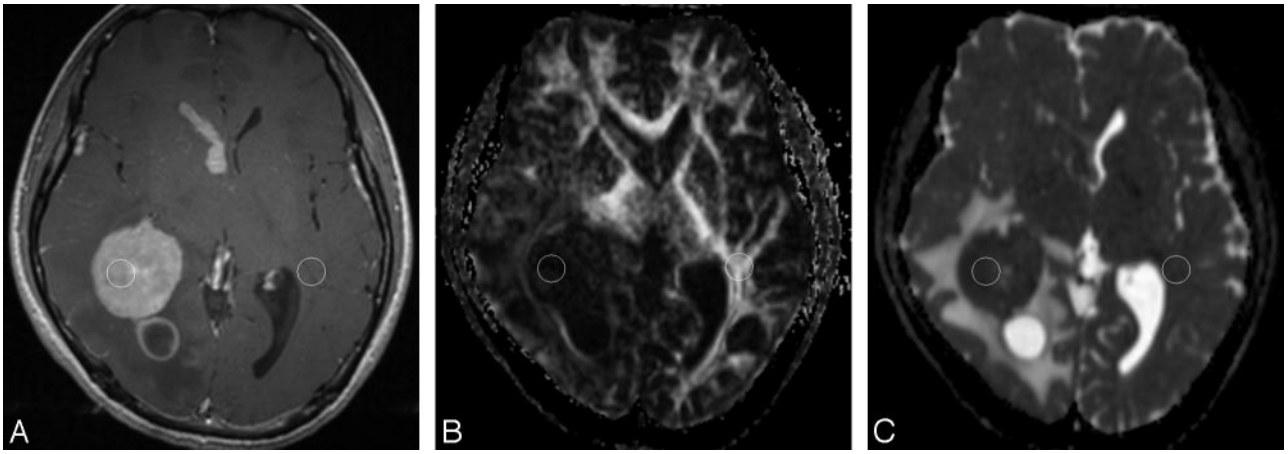


**Fig 1.** ADC and FA measurements in a 22-year-old man with pathologically confirmed lymphoma in the right temporo-occipital region. *A*, Axial contrast-enhanced T1-weighted MR image (781/8.1) shows an enhancing mass in the right temporo-occipital region. There are enhancing nodules along the right frontal ependymal surface. There is a rim-enhancing nodule posteromedial to the main mass; cystic change or necrosis of the tumor is considered. One ROI is in the enhancing tumor area for measurement of ADC and FA values, and another ROI is at a corresponding site in the contralateral NAWM. On FA (*B*) and ADC (*C*) maps, the ROIs in *A* are superimposed.

weighted imaging (T1WI) performed before and after intravenous administration of 0.1 mmol/kg of body weight of gadopentetate dimeglumine (Magnevist; Schering, Berlin, Germany). All of the MR imaging studies were performed as a single MR imaging investigation on a 3T MR imaging unit (Magnetom Triotim; Siemens, Erlangen, Germany). DTI was performed in the axial plane using single-shot echo-planar imaging with the following parameters: TR, ms/TE ms, 8600/91; diffusion gradient encoding in 12 directions; $b = 0$; 1000 s/mm$^2$; FOV, 192 × 192 mm; matrix size, 128 × 128; section thickness, 3 mm; and number of signal intensity acquired, 5. A total of 35–40 sections covered the cerebral hemispheres, upper brain stem, and cerebellum without gaps. To minimize artifacts such as signal intensity dropout and gross geometric distortions associated with the echo-planar imaging, parallel imaging technique (generalized autocalibrating partially parallel acquisitions[24]; reduction factor = 2) was used during DTI acquisitions. Immobilization of the patient's head to minimize artifacts due to patient motion was achieved by fixation of the head in a headrest.

### *Image Postprocessing*

The diffusion-tensor data were transferred to an independent workstation and processed using the software nordicICE (Nordic Image Control and Evaluation Version 2.16; Nordic Imaging Lab, Bergen, Norway). Voxel by voxel, the FA and directionally averaged ADC (also known as mean diffusivity) were calculated by using the following standard algorithms:

$$1)\qquad ADC = \bar{\lambda} = \frac{\lambda_1 + \lambda_2 + \lambda_3}{3}$$

and

$$2)\qquad FA = \sqrt{\frac{3}{2}} \cdot \sqrt{\frac{(\lambda_1 - \bar{\lambda})^2 + (\lambda_2 - \bar{\lambda})^2 + (\lambda_3 - \bar{\lambda})^2}{\lambda_1^2 + \lambda_2^2 + \lambda_3^2}},$$

where $\lambda_n$ is the eigenvalue describing a diffusion tensor.

### *Visual Inspection*

Two experienced neuroradiologists performed qualitative visual inspection of FA maps of lymphomas and GBMs with consensus reading. Each lesion was evaluated as being predominantly hyperintense, isointense, or hypointense relative to white matter, and the findings were recorded.

### *FA and ADC Measurement*

Using the coregistration module integrated in the software nordicICE, the FA and ADC maps were automatically coregistered to postcontrast T1WI based on Digital Imaging and Communications in Medicine geometry parameters. The adequacy of registration was assessed with visual inspection by the 2 observers. Manual adjustment of image registration was performed if necessary. Circular regions of interest (ROIs) with diameter ranges from 0.7 to 1.2 cm were randomly placed centrally within the largest solid-enhancing area of all lymphomas (Fig 1) and GBMs (Fig 2) to avoid volume averaging with cystic or necrotic regions that might influence FA and ADC values. Because it is often possible to differentiate between lymphomas and GBMs on conventional imaging, neuroradiologists placing the ROIs were not blinded to the diagnosis. The ROIs were then automatically transferred to the coregistered ADC and FA maps. Approximate same-size ROIs were also drawn in matching structures in the contralateral hemisphere in each patient to obtain FA and ADC values of normal-appearing white matter (NAWM) for the purpose of normalization. The matching white matter structure represented the same structure in the contralateral hemisphere.

### *Statistical Analysis*

Mean FA and ADC values were evaluated for each ROI. The FA and ADC ratios were calculated by dividing the FA and ADC values in the solid-enhancing areas of lymphomas and GBMs by the FA and ADC values of NAWM in the contralateral hemisphere in the same patient. Comparisons between solid-enhancing areas of lymphoma or GBM and the corresponding contralateral NAWM were performed by using paired *t* tests. The mean FA and FA ratios, ADC, and ADC ratios of the solid-enhancing areas for the 2 tumor groups were compared with a 2-sample *t* test. Cutoff values of FA, FA ratio, ADC, and ADC ratio for distinguishing lymphomas from GBMs were determined by receiver operating characteristic (ROC) curve analysis. The ROC curve was further used to calculate the area under the curve (AUC) value, which is an index of overall discriminative ability of a given method. A commercially available statistical software package (SPSS 15; SPSS Chicago, Ill) was used for analysis, and $P$ values $< .05$ were considered to indicate a statistically significant difference.

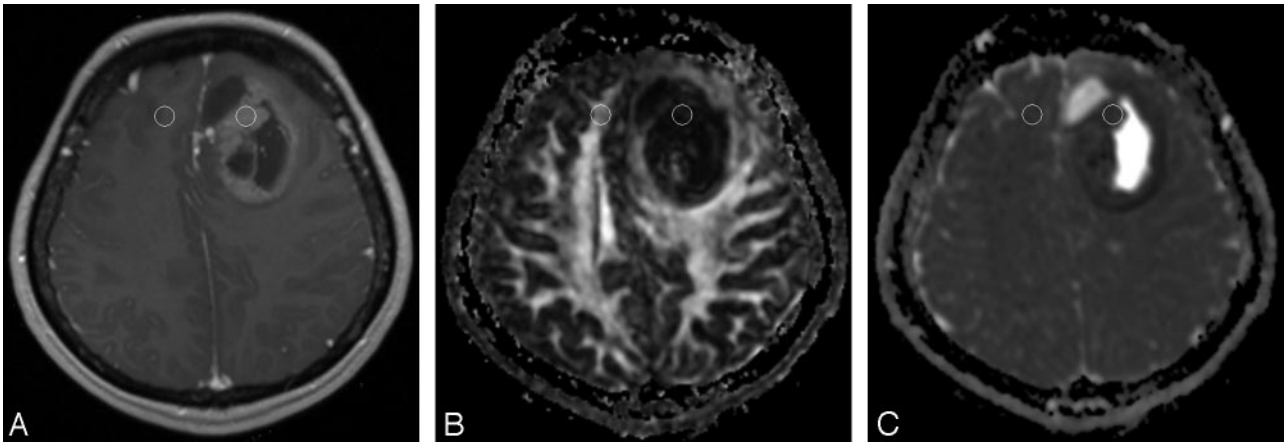


**Fig 2.** ADC and FA measurements in a 45-year-old woman with pathologically confirmed GBM in the left frontal region. *A*, Axial contrast-enhanced T1-weighted MR image (350/2.5) shows an enhancing mass in the left frontal region. One ROI is in the enhancing tumor area for measurement of ADC and FA values, and another ROI is at a corresponding site in the contralateral NAWM. On FA (*B*) and ADC (*C*) maps, the ROIs in *A* are superimposed.

**Table 1: ADC, ADC ratios, FA, and FA ratios of lymphoma and GBM**

| Variable | Lymphoma | GBM | *P* | 95% CI |
|---|---|---|---|---|
| FA | 0.140 ± 0.024 | 0.229 ± 0.069 | .001 | −0.137 to −0.040 |
| FA ratios | 0.25 ± 0.04 | 0.40 ± 0.12 | .002 | −0.234 to −0.064 |
| ADC ($\times 10^{-3}$ mm$^2$/s) | 0.630 ± 0.155 | 0.963 ± 0.119 | <.001 | −0.463 to −0.203 |
| ADC ratios | 0.83 ± 0.14 | 1.26 ± 0.13 | <.001 | −0.558 to −0.304 |

**Note:**—Data are the mean ± SD. FA indicates fractional anisotropy; ADC, apparent diffusion coefficient; GBM, glioblastoma multiforme; CI, confidence interval. ADC and FA ratios were calculated by dividing the mean ADC or FA values of the affected hemisphere by those of the normal-appearing white matter of the contralateral hemisphere.

## Results

### *Visual Inspection*

All of the lymphomas and GBM appeared predominantly hypointense relative to white matter on FA maps.

### *Mean FA Values and FA Ratios*

The mean FA values of lymphoma and contralateral NAWM were 0.140 ± 0.024 (range, 0.092–0.170) and 0.565 ± 0.028 (range, 0.523–0.599), respectively ($P < .001$). The mean FA values of GBM and contralateral NAWM were 0.229 ± 0.069 (range, 0.179–0.285) and 0.584 ± 0.034 (range, 0.525–0.632), respectively ($P < .001$). The mean FA values of lymphomas were significantly lower than those in GBM ($P = .001$; Table 1). The mean FA values of contralateral NAWM of lymphomas were not significantly different from those of GBM ($P = .198$). The mean FA ratios were 0.25 ± 0.04 (range, 0.17–0.29) for those with lymphomas and 0.40 ± 0.12 (range, 0.15–0.59) for those with GBM ($P = .002$; Table 1). The changes in FA in solid-enhancing areas of lymphoma and GBM and NAWM were plotted against ADC (Fig 3).

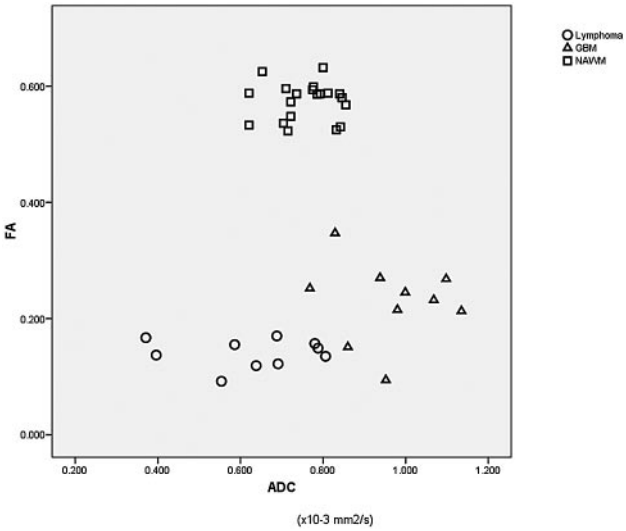


**Fig 3.** Scatterplot of FA versus ADC measured in solid enhancing tumors and contralateral NAWM. Measurements from lymphomas tend to cluster in the area corresponding with FA and ADC decreases, whereas measurements from GBMs tend to cluster in area corresponding with FA decreases and ADC increases.

### *Mean ADC Values and ADC Ratios*

The mean ADC values ($\times 10^{-3}$ mm$^2$/s) of lymphoma and contralateral NAWM were 0.630 ± 0.155 (range, 0.371–0.806) and 0.752 ± 0.086 (range, 0.621–0.846), respectively ($P = .003$). The mean ADC values ($\times 10^{-3}$ mm$^2$/s) of GBM and contralateral NAWM were 0.963 ± 0.119 (range, 0.768–1.135) and 0.764 ± 0.063 (range, 0.653–0.855), respectively ($P < .001$). The mean ADC values of lymphomas were significantly lower than those in GBM ($P < .001$). The mean ADC values of contralateral NAWM of lymphomas were not significantly different from those of GBM ($P = .712$). The mean ADC ratios were 0.83 ± 0.14 (range, 0.55–0.97) for those with lymphomas and 1.26 ± 0.13 (range, 1.09–1.46) for those with GBM ($P < .001$; Table 1).

### *ROC Curve Analysis*

The optimal cutoff values for differentiating lymphomas from GBM were 0.192 (sensitivity, 100%; specificity, 80%; accuracy, 90%) for FA, 0.33 (sensitivity, 100%; specificity, 80%; accuracy, 90%) for FA ratio, 0.818 × $10^{-3}$ mm$^2$/s (sensitivity, 100%; specificity, 90%; accuracy, 95%) for ADC, and 1.06 (sensitivity, 100%; specificity, 100%; accuracy, 100%) for

**Table 2: Measures of sensitivity, specificity, and accuracy in discrimination of lymphomas from GBMs with receiver operating characteristic curve analysis**

| Variable | CV | Sensitivity, % | Specificity, % | Accuracy, % | AUC, % | *P* |
|---|---|---|---|---|---|---|
| FA | 0.192 | 100 | 80 | 90 | 0.87 | .005 |
| FA ratios | 0.330 | 100 | 80 | 90 | 0.84 | .010 |
| ADC | 0.818 | 100 | 90 | 95 | 0.97 | <.001 |
| ADC ratios | 1.060 | 100 | 100 | 100 | 1.00 | <.001 |

**Note:**—FA indicates fractional anisotropy; ADC, apparent diffusion coefficient; GBM, glioblastoma multiforme; CV, cutoff value; AUC, area under the curve.

ADC ratio. ADC, in absolute values and ratios, was more specific and accurate than FA in discriminating lymphomas from GBMs. The sensitivity of FA and ADC, on the other hand, was not different in differentiating the 2 tumors (Table 2). The discriminative ability of these diffusion tensor metrics to differentiate 2 tumor types, in decreasing order of AUC value, were ADC ratio (AUC, 1), ADC value (AUC, 0.97), FA value (AUC, 0.87), and FA ratio (AUC, 0.84).

## Discussion

Our study showed that all of the lymphomas were predominantly hypointense on FA maps of DTI and showed significant FA decreases in solid-enhancing areas compared with contralateral NAWM. The FA and ADC of lymphomas were significantly lower than those in the GBM.

In our study, FA and ADC values obtained in NAWM and solid-enhancing areas of GBM correlated well with those reported for GBM.[17-19] Our quantitative measurements of ADC and FA in solid-enhancing areas of GBM showed increased ADC values (mean percentage of 126% of contralateral NAWM) and decreased FA values (40% of normal value), which were similar to previous studies.[4,5,17-19] ADC values obtained in NAWM and solid-enhancing areas of lymphoma[3-5,19] also correlated well with those reported in the literature. However, no qualitative or quantitative FA changes for lymphoma are available from published studies for comparison.

In our study, the mean ADC values of lymphomas were significantly lower than those of NAWM and GBM, findings that were consistent with the higher cellularity in the lymphoma. This inverse relationship between the ADC values and cellularity has been reported previously in gliomas and lymphomas.[4] In contrast, there is still controversy regarding the relationship between FA and tumor cellularity. Beppu and colleagues[21-23] reported a positive correlation of FA value with glial tumor cellularity, that is, higher FA was associated with higher tumor cellularity. In a more recent study, a negative relationship was found when FA changes were correlated with cellularity as determined histologically.[20] Our results show that FAs of lymphomas, which have higher cellularity, were lower than those of GBM, and suggest that FA is inversely related to cellularity.

The actual mechanism for FA decrease in brain tumors is still unclear. Some researchers[17,25,26] have suggested that the FA decrease is related to an increase in extracellular space secondary to neuronal and fiber tract destruction. Other investigators[20] proposed that low FA is related to a decrease in extracellular space secondary to tumor infiltration when they observed a negative relationship between FA and tumor cellularity. We think that the FA decrease in lymphoma is related to decreased extracellular space secondary to attenuated tumor growth.

In our study, ADC and FA have similar sensitivity in differentiating lymphomas from GBMs. The specificity and accuracy of ADC, however, were higher than those of FA in differentiating the two. In a previous study, ADC was 90% accurate and 100% specific in differentiating between lymphomas and GBMs.[27] Our results agree with those of the previous report. The high specificity and accuracy of ADC in differentiating lymphoma from GBM are probably due to the differences in tumor cellularity, which has been considered the primary determinant of ADC.[7] In contrast to ADC that measures the magnitude of molecular motion of water and does not depend directly on the integrity of myelinated fiber tracts, FA depends on the restriction of water proton movement along myelinated fiber tracts.[28] The assessment of diffusion anisotropy in tumor tissue is a complicated issue, which is affected by the ratio of extracellular to intracellular space, vascularity, edema, microcysts, and extracellular matrix.[25,29-32] We speculate that the complexity of diffusion anisotropy determination renders FA to be a less specific and less accurate tensor metric than ADC in distinguishing lymphomas from GBMs.

Although FA is slightly less specific and less accurate than ADC in differentiating lymphoma from GBM, its overall discriminating ability in both absolute value and ratio is good with AUC $>$ 0.85, sensitivity 100%, specificity 80%, and accuracy 90%, respectively. A previous study showed that there is no correlation between FA and ADC measurements in structural abnormalities and, thus, ADC and FA may be independent.[26] Therefore, FA may serve as an independent diagnostic criterion or, when combined with the results of ADC, further improve the diagnostic accuracy in the differentiation of lymphoma and GBM. Further studies are needed to support our speculations.

There are limitations to our study. First, we did not compare the cellularity or other histologic changes in lymphoma and GBM, and, therefore, we cannot definitively state that the FA decreases and differences between lymphoma and GBM were due to differences in cellularity and the size of extracellular space. Second, the DTI findings of brain tumors and the relationship between FA and tumor cellularity reported previously were primarily observed in glial tumors, and, thus, conclusions from previous studies regarding FA changes in gliomas may not be applicable to lymphoma. Third, the small number of patients in our study is recognized as another limitation, particularly in performing ROC curve analysis. Therefore, the sensitivity, specificity, and accuracy of each tensor metric may be different as the number of patients increases. Despite these limitations, the FA decreases in lymphoma, as

well as differences between lymphoma and GBM on DTI, were unequivocally demonstrated in our study.

## Conclusion

Primary cerebral lymphoma shows the FA decrease compared with NAWM. The FA and ADC of primary cerebral lymphoma were significantly lower than those of GBM. DTI is able to differentiate lymphomas from GBM.

## References


1. Surawicz TS, McCarthy BJ, Kupelian V, et al. **Descriptive epidemiology of primary brain and CNS tumors: results from the Central Brain Tumor Registry of the United States, 1990–1994**. *Neuro-oncol* 1999;1:14–25
2. Stadnik TW, Demaerel P, Luypaert RR, et al. **Imaging tutorial: differential diagnosis of bright lesions on diffusion-weighted MR images**. *Radiographics* 2003;23:e7
3. Stadnik TW, Chaskis C, Michotte A, et al. **Diffusion-weighted MR imaging of intracerebral masses: comparison with conventional MR imaging and histologic findings**. *AJNR Am J Neuroradiol* 2001;22:969–76
4. Guo AC, Cummings TJ, Dash RC, et al. **Lymphomas and high-grade astrocytomas: comparison of water diffusibility and histologic characteristics**. *Radiology* 2002;224:177–83
5. Yamasaki F, Kurisu K, Satoh K, et al. **Apparent diffusion coefficient of human brain tumors at MR imaging**. *Radiology* 2005;235:985–91
6. Sugahara T, Korogi Y, Kochi M, et al. **Usefulness of diffusion-weighted MRI with echo-planar technique in the evaluation of cellularity in gliomas**. *J Magn Reson Imaging* 1999;9:53–60
7. Kono K, Inoue Y, Nakayama K, et al. **The role of diffusion-weighted imaging in patients with brain tumors**. *AJNR Am J Neuroradiol* 2001;22:1081–88
8. Chang YW, Yoon HK, Shin HJ, et al. **MR imaging of glioblastoma in children: usefulness of diffusion/perfusion-weighted MRI and MR spectroscopy**. *Pediatr Radiol* 2003;33:836–42
9. Batra A, Tripathi RP. **Atypical diffusion-weighted magnetic resonance findings in glioblastoma multiforme**. *Australas Radiol* 2004;48:388–91
10. Hakyemez B, Erdogan C, Yildirim N, et al. **Glioblastoma multiforme with atypical diffusion-weighted MR findings**. *Br J Radiol* 2005;78:989–92
11. Toh CH, Chen YL, Hsieh TC, et al. **Glioblastoma multiforme with diffusion-weighted magnetic resonance imaging characteristics mimicking primary brain lymphoma. Case report.** *J Neurosurg* 2006;105:132–35
12. Baehring JM, Bi WL, Bannykh S, et al. **Diffusion MRI in the early diagnosis of malignant glioma**. *J Neurooncol* 2007;82:221–25
13. Wiegell MR, Larsson HBW, Wedeen VJ. **Fiber crossing in human brain depicted with diffusion tensor MR imaging**. *Radiology* 2000;217:897–903
14. Le Bihan D, van Zijl P. **From the diffusion coefficient to the diffusion tensor**. *NMR Biomed* 2002;15:431–34
15. Hansen JR. **Pulsed NMR study of water mobility in muscle and brain tissue**. *Biochim Biophys Acta* 1971;230:482–86
16. Chenevert TL, Brunberg JA, Pipe JG. **Anisotropic diffusion in human white matter: demonstration with MR techniques in vivo**. *Radiology* 1990;177:401–05
17. Sinha S, Bastin ME, Whittle IR, et al. **Diffusion tensor MR imaging of high-grade cerebral gliomas**. *AJNR Am J Neuroradiol* 2002;23:520–27
18. Lu S, Ahn D, Johnson G, et al. **Diffusion-tensor MR imaging of intracranial neoplasia and associated peritumoral edema: introduction of the tumor infiltration index**. *Radiology* 2004;232:221–28
19. Provenzale JM, McGraw P, Mhatre P, et al. **Peritumoral brain regions in gliomas and meningiomas: investigation with isotropic diffusion-weighted MR imaging and diffusion-tensor MR imaging**. *Radiology* 2004;232:451–60
20. Stadlbauer A, Ganslandt O, Buslei R, et al. **Gliomas: histopathologic evaluation of changes in directionality and magnitude of water diffusion at diffusion-tensor MR imaging**. *Radiology* 2006;240:803–10
21. Beppu T, Inoue T, Shibata Y, et al. **Measurement of fractional anisotropy using diffusion tensor MRI in supratentorial astrocytic tumors**. *J Neurooncol* 2003;63:109–16
22. Inoue T, Ogasawara K, Beppu T, et al. **Diffusion tensor imaging for preoperative evaluation of tumor grade in gliomas**. *Clin Neurol Neurosurg* 2005;107:174–80
23. Beppu T, Inoue T, Shibata Y, et al. **Fractional anisotropy value by diffusion tensor magnetic resonance imaging as a predictor of cell density and proliferation activity of glioblastomas**. *Surg Neurol* 2005;63:56–61
24. Bhagat YA, Emery DJ, Naik S, et al. **Comparison of generalized autocalibrating partially parallel acquisitions and modified sensitivity encoding for diffusion tensor imaging**. *AJNR Am J Neuroradiol* 2007;28:293–98
25. Brunberg JA, Chenevert TL, McKeever PE, et al. **In vivo MR determination of water diffusion coefficients and diffusion anisotropy: correlation with structural alteration in gliomas of the cerebral hemispheres** [**published correction appears in *AJNR Am J Neuroradiol* 1995;16:1384**]. *AJNR Am J Neuroradiol* 1995;16:361–71
26. Wieshmann UC, Clark CA, Symms MR, et al. **Reduced anisotropy of water diffusion in structural cerebral abnormalities demonstrated with diffusion tensor imaging**. *Magn Reson Imaging* 1999;17:1269–74
27. Al-Okaili RN, Krejza J, Woo JH, et al. **Intraaxial brain masses: MR imaging-based diagnostic strategy–initial experience**. *Radiology* 2007;243:539–50
28. Le Bihan D, Mangin J-F, Poupon C, et al. **Diffusion tensor imaging: concepts and applications**. *J Magn Reson Imaging* 2001;13:534–46
29. Latour LL, Svoboda K, Mitra PP, et al. **Time-dependent diffusion of water in a biological model system**. *Proc Natl Acad Sci U S A* 1994;91:1229–33
30. Garcia-Perez AI, Lopez-Beltran EA, Kluner P, et al. **Molecular crowding and viscosity as determinants of translational diffusion of metabolites in subcellular organelles**. *Arch Biochem Biophys* 1999;362:329–38
31. Tanner JE. **Intracellular diffusion of water**. *Arch Biochem Biophys* 1983;224:416–28
32. Szafer A, Zhong J, Anderson AW, et al. **Diffusion-weighted imaging in tissues: theoretical models**. *NMR Biomed* 1995;8:289–96